Design and Realization of a Low Cross-Polarization Conical Horn With Thin Metasurface Walls

Valentina Sozio, Enrica Martini, *Senior Member, IEEE*, Francesco Caminita, Paolo De Vita, Marco Faenzi, Andrea Giacomini, *Member, IEEE*, Marco Sabbadini, Stefano Maci, *Fellow, IEEE*, and Giuseppe Vecchi, *Fellow, IEEE*

***Abstract*— A *Ku*-band low cross-polarization conical horn based on thin metasurface (MTS) walls is presented in this article, along with the relevant design method. The necessary boundary conditions are realized by printing a tensor MTS on the internal walls of the horn, which yields a radiation performance similar to a standard corrugated Gaussian horn yet with the benefits of thin walls. The design method is based on the adiabatic approximate solution for the hybrid mode of a conical waveguide with generic balanced impedance walls, which allows the determination of the impedance profile supporting a single balanced mode. The impedance design is based on the usual locally flat approximation of the wall and on the assumption of plane wave incidence. This approach results in an analytic design method that requires no optimization. The design has been first validated by solving the problem with homogenized impedance boundary conditions through a body of revolution (BoR) method of moments. The actual structure, including impedance wall implementation, is then simulated in full detail with a full-wave fast code. Finally, the horn has been realized and experimentally characterized; measurements show excellent agreement both with theory and with simulations, with a cross-polarization level below −20 dB over a 2 GHz bandwidth.**

***Index Terms*— Horn antennas, hybrid modes, metasurfaces (MTSs), modal analysis, surface impedance.**

I. Introduction

HORN antennas with symmetric radiation properties and low cross-polarization for an efficient illumination of reflector antennas have been under investigation since the 1960s. Smooth wall circular horns can be designed by combining two modes [1], achieving axial symmetry and low cross-polarization in the radiation pattern but limited bandwidth as a drawback. The advent of corrugated horns [2], [3] has overcome the narrow band issue, still maintaining axial beam symmetry, low side lobes, and low cross-polarization, thus representing a milestone in the history of horn feeds [4].

In [3], it is demonstrated that symmetric patterns can be obtained with HE/EH hybrid modes . Anisotropic impedance boundary conditions (AIBCs) at the horn walls are required to support these hybrid modes. In particular, surface impedances must satisfy the so-called "balanced" hybrid condition to ensure low (theoretically zero) cross-polarization. An "artificial" surface is, therefore, needed to achieve this condition [5]. Corrugations (with dielectric filling material), both transverse and longitudinal to the direction of the wave, are the most known and largely used implementations of these artificial surfaces. Referring to the boundary conditions in acoustic, transversely and longitudinally corrugated surfaces have been described as artificial soft and hard surfaces, respectively [6]. In [7], these concepts are applied to the design of hybrid-mode horn antennas.

Soft and hard AIBCs are special cases of the balanced hybrid condition: soft horns assure low sidelobes but low gain and hard horns have high gain but also high sidelobe level; a compromise with a good gain and an acceptable sidelobe level can be achieved by using finite wall impedances that respect the balanced hybrid condition. Soft hybrid mode horns have been designed with foam or solid dielectric cores (one or two) and strip-loaded walls; and hard hybrid mode horns have been realized with strip-loaded walls with and without vias, or with two dielectric cores (see [8] for a complete review about soft and hard horn antennas).

The development of dual dielectric-core horn antennas capable of being designed to satisfy any (balanced) AIBCs between the soft and hard one first appears in [9] and [10]. However, dielectric-loaded horns are characterized by heavy weight and high losses.

The advent of metamaterials (MTMs) and metasurfaces (MTSs) and their increasing comprehension have inspired the realization of synthetic surfaces for symmetric pattern horn antennas [11]. An approach based on metasurfing [12] has been used to address sectoral H-plane horns [13]. In [14], hybrid-mode soft and hard horn antennas are designed for the first time with an ideal low-index MTM wall, as an

Manuscript received May 28, 2019; revised November 20, 2019; accepted December 22, 2019. Date of publication February 26, 2020; date of current version May 5, 2020. This work was supported by the Italian Space Agency (ASI) in the framework of the ARTES Program through the European Space Agency (ESA) under Contract 4000113142/15/NL/IA. *(Corresponding author: Stefano Maci.)*

Valentina Sozio was with Links Foundation, 10138 Torino, Italy. (e-mail: valentina.sozio@virgilio.it).

Enrica Martini, Marco Faenzi, and Stefano Maci are with the Department of Information Engineering and Mathematics, University of Siena, 53100 Siena, Italy (e-mail: martini@dii.unisi.it; faenzi@diism.unisi.it; macis@dii.unisi.it).

Francesco Caminita is with Wave Up Srl, 53100 Siena, Italy (e-mail: francesco.caminita@wave-up.it).

Paolo De Vita is with Ingegneria dei Sistemi (IDS), 56121 Pisa, Italy (e-mail: p.devita@idscorporation.com).

Andrea Giacomini is with Microwave Vision Italy s.r.l., 00071 Pomezia, Italy (e-mail: andrea.giacomini@mvg-world.com).

Marco Sabbadini was with the Antenna and Sub-Millimetre Waves Section, Radio Frequency Payloads and Technology Division, ESA – ESTEC, NL-2200 AG Noordwijk, The Netherlands. He is now with the University of Siena, 53100 Siena, Italy (e-mail: marco.sabbadini@ziggo.nl).

Giuseppe Vecchi is with the Department of Electronics and Telecommunications, Politecnico di Torino, 10144 Torino, Italy (e-mail: giuseppe.vecchi@polito.it).

Color versions of one or more of the figures in this article are available online at http://ieeexplore.ieee.org.

Digital Object Identifier 10.1109/TAP.2020.2975253

attractive alternative to the dual dielectric-core horns. In [15], MTS walls, implemented with metallic FSS type screens and vias on a grounded dielectric layer, are engineered with a genetic algorithm optimization to provide soft, hard, and balanced hybrid conditions in conical horn antennas over a wide bandwidth. The design is corroborated by full-wave simulations. In [16], MTS impedance tapering is introduced to improve radiation characteristics and impedance matching over a broader bandwidth; also in this case, the design is verified through simulations. The impedance tapering profile in [16] is determined through an optimization procedure based on the full-wave analysis of the whole horn structure. However, this kind of optimization can be very time consuming. On the other hand, a design approach based on a quasi-analytical modal analysis (similar to what is done for corrugated horns) has the advantage to be computationally inexpensive, while providing a physical insight into the horn behavior.

In this article, a modal field-based method [7], [17]–[19] is applied for the design of low cross-polarization conical horns with engineered MTSs walls. As it is well known, the definition of modes in a structure requires the separability of the wave equation and of the BCs in the appropriate coordinate system. In a conical waveguide with impedance walls, separability is possible only for perfect electric conductor/perfect magnetic conductor (PEC/PMC) BCs and, approximately, for soft/hard cases. The latter are important, since they model conical corrugated horns [4], [17], [18].

The conical mode analysis has also been extended in the adiabatic approximation to conical horns with arbitrary wall impedances [7]. This will be our starting point to develop an analytical-based design method for this class of horns.

This article is structured as follows. Section II presents the conical adiabatic mode solution for impedance walls, and its use on a truncated conical horn. A numerical validation supporting the theoretical considerations is presented through a body of revolution Method of Moments (MoM) analysis with the use of realistic homogenized boundary conditions. Section III presents the low cross-polarization metahorn design, including implementation of the theoretical AIBC through subwavelength slotted patches, and the numerical full-wave results of the detailed antenna structure. Section IV presents manufacturing and measurements of the antenna. Finally, conclusions are drawn in Section V.

II. Conical Modes for Impedance Walls

A metahorn is a metallic horn antenna whose interior walls are coated with a dielectric material printed with a metallic texture consisting of subwavelength patches, as shown in Fig. 1. A spherical coordinate system (r, θ, ϕ) is introduced as depicted there, where r is the radial distance from the cone vertex. We denote with a and w_g the radii of the largest and the smallest circular sections of the horn, respectively, and with θ_1 the half flare angle.

The MTS is effectively modeled in terms of an equivalent anisotropic impenetrable IBC [20], characterized by a diagonal tensor, whose matrix representation in spherical coordinates is

$$\underline{\underline{Z}} = \begin{bmatrix} Z_r & 0 \\ 0 & Z_\phi \end{bmatrix}. \tag{1}$$

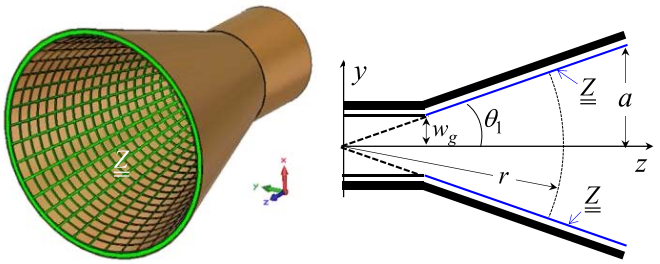

Fig. 1. Pictorial representation of the MTS horn, and geometry of its longitudinal cross section.

All the entries are purely reactive in the absence of losses, as implied in the following.

A. Characteristic Equation

Separation of variables, as described in [7], [17], and [18], yields the characteristic equation for the conical modes [19]. As a consequence of the periodicity condition dictated by the rotational symmetry of the horn structure, the azimuthal index must be an integer number. We denote this number by m. For any m, the noninteger radial index ν depends on the flare angle θ_1 and on the impedance entries via the following characteristic equation:

$$\left(p_\nu^m(\theta_1) - \frac{\nu(\nu+1)}{jkr\eta_0} Z_\phi\right) \cdot \left(p_\nu^m(\theta_1) - \frac{\nu(\nu+1)\eta_0}{jkr}(Z_r)^{-1}\right) = -\left(\frac{m h_\nu(kr)}{\sin\theta_1}\right)^2 \tag{2}$$

where η_0 and k denote the free-space characteristic impedance and wavenumber, respectively, and $h_\nu(x) = [d\hat{H}_\nu^{(2)}(x)/dx]/\hat{H}_\nu^{(2)}(x)$, where $\hat{H}_\nu^{(2)}(x)$ is the Schelkunoff Hankel function of second kind and order ν. In (2), $p_\nu^m(\theta) = [dP_\nu^m(\cos\theta)/d\theta]/P_\nu^m(\cos\theta)$, where $P_\nu^m(\cos\theta)$ is the associated Legendre function of order m and degree ν. We note that the computation of the associated Legendre function requires the use of hypergeometric functions [21], [22].

B. Adiabatic Solution

A generic modal function solution of (2) is of the kind $F_{m\nu}(r, \theta_1)$. In this context, the presence of the radial coordinate r in the characteristic equation is a well-known problem, since it does not allow for an exact solution in the general case. This problem can be circumvented by resorting to the so-called "adiabatic" approximation,[1] which consists in considering the radial index to be a function of the radial position r via the solution of (2), i.e., $\nu = \nu(kr)$.

It is of interest to study the case $kr \gg \nu$, for which the radial function simplifies to its asymptotic *constant* expression

[1] In [23] and [24], a modal field-based approach, based on the definition of "adiabatic modes," and their extension to "intrinsic modes" were presented as solution to propagation problems when separability conditions are not completely matched along the z axes. The work presented in those references was relevant to cylindrical structures which exhibit a local longitudinal variation of boundary conditions. Along a similar guideline, we use here an "adiabatic concept" to study the exact characteristic equation for conical boundaries.

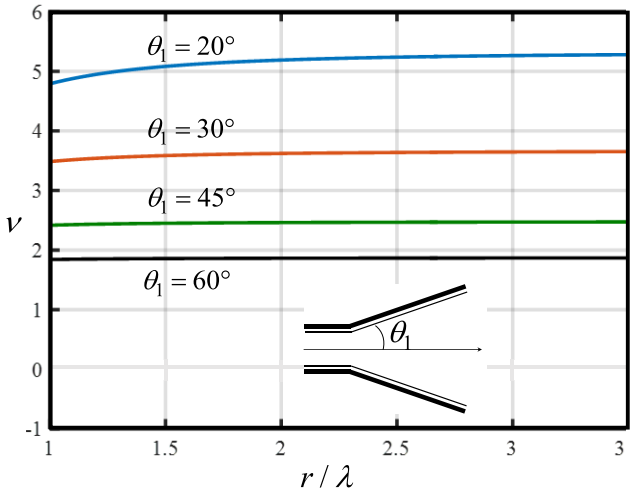

Fig. 2. Solution of (2) obtained with the use of (3) for various values of the flare angle and for $C = 0.06$.

$h_\nu(kr) \approx -j$. In this case, it is apparent from (2) that the solution for ν is independent of the position r only if the impedance profile is of the kind

$$Z_\varphi(r) = j\frac{\eta_0 r}{C}; \quad Z_r(r) = -j\frac{\eta_0 C}{r} \tag{3}$$

where C is an arbitrary real constant. It is worth noting that in this case

$$Z_\varphi(r) \cdot Z_r(r) = \eta_0^2 \tag{4}$$

which is the well-known balanced condition that ensures zero cross-polarization [3], [25]. We note that this condition is also the same obtained in [15] and [16] for conical balanced horns and in [26] for dual polarization mode in MTS antennas. Since in the absence of losses the impedance entries are purely imaginary, (3) implies an opposite capacitive or inductive nature of the two impedances, together with a specific opposite dependence on r. This dependence is the first key point in our method. In fact, for $kr \gg \nu$, condition (3) leads to the following simple asymptotic form of the characteristic equation:

$$\left(p_\nu^m(\theta_1) - \frac{\nu(\nu+1)}{Ck}\right)^2 = \left(\frac{m}{\sin\theta_1}\right)^2 \quad kr \gg \nu \tag{5}$$

the solution of which is independent of r, as occurs for conical modes in the presence of PEC walls. It is, therefore, expected that the solution of the characteristic equation (2) under the balanced condition (3) is weakly dependent on r, becoming asymptotically constant for kr large. This is indeed observed in Fig. 2, where the solution of (2) for $m = 1$ (dominant mode) is plotted as a function of r/λ for various flare angles. For increasing flare angles, ν reaches its asymptotic value more rapidly. It is also worth noting that very close to the horn vertex (origin of the reference system), a very small imaginary part of ν is found for small flare angle, not depicted in Fig. 2.

C. Local Incidence Angle

The smooth radial dependence of the radial index legitimates the mentioned local adiabatic solution $\nu(kr)$ obtained

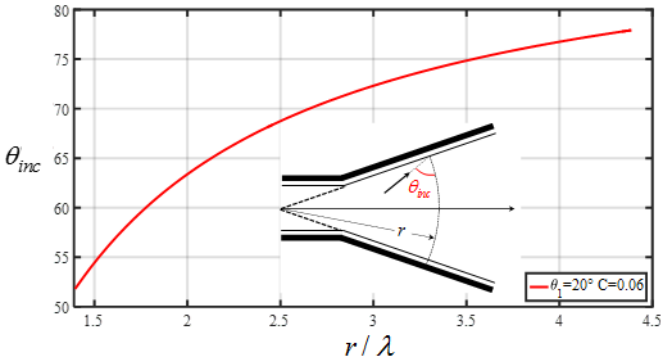

Fig. 3. Incidence angle as a function of the normalized radial position for a flare angle of the horn equal to 20° and $C = 0.06$, under balanced hybrid condition (3).

solving the characteristic equation of the conical section by section and the use of it as a basic input for the MTS design. In doing that, it is important to account for the space dispersivity of the homogenized impedance for the practical realization of the MTS with printed texture.

To this end, we assume that the local modal incidence angle is

$$\theta_{inc} = \arcsin\left\{\Re\mathrm{e}\left(\frac{k_r(r)}{k}\right)\right\} \tag{6}$$

where $k_r(r)$ is the normalized radial wavenumber of the mode, namely [4], [17]

$$\frac{k_r(r)}{k} = jh_\nu(kr) = j\frac{\frac{\partial}{\partial kr}\hat{H}_\nu^{(2)}(kr)}{\hat{H}_\nu^{(2)}(kr)} = j\frac{\partial\left[\ln \hat{H}_\nu^{(2)}(kr)\right]}{\partial kr}. \tag{7}$$

An example of the dependence of incidence angle on the radial position is shown in Fig. 3.

D. Impenetrable Impedance Versus Penetrable Impedance

The knowledge of the incidence angle, together with (3), is the second key point for the MTS synthesis. It is indeed well known [20], [27] that an MTS realized by printed elements over a grounded slab can be modeled by an "impenetrable" surface impedance, but the resulting value is dependent on the local wave vector. This is because the homogenized impedance takes into account the contribution of both the grounded dielectric slab, typically wavevector dependent (and therefore requiring the knowledge of the local incidence angle, identified by **Errore. L'origine riferimento non è stata trovata**. in our method), and the homogenized "penetrable" impedance associated with the printed metallization. The latter is almost independent of the wave vector in a broad frequency range. The resulting combination of the two contributions, approximated through a local transmission line model, leads to the impenetrable impedance.

Examples of opaque (impenetrable) reactances X_ϕ, X_r and transparent (penetrable) reactances X_ϕ^{transp}, X_R^{transp} are plotted in Fig. 4 as a function of the normalized radial distance. The dielectric substrate selected for the MTS metallic printing has a thickness of $h_d = 1.016$ mm and a permittivity of $\varepsilon_r = 3.6$. The example is relevant to a conical horn working at 12 GHz with a flare angle 18.445°. The surface impedances are defined

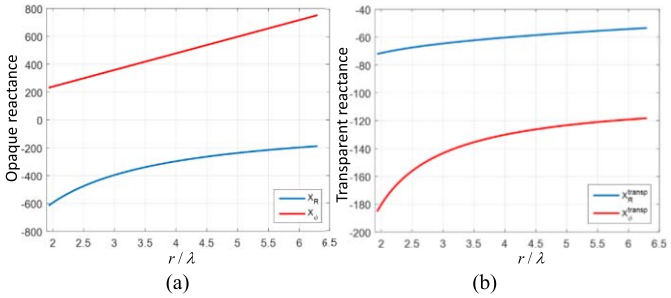

Fig. 4. (a) Impenetrable reactances and (b) penetrable reactances versus the radial distance from the horn vertex. Note the different ranges in the vertical scale.

through (3) with $C = 0.0788$ in order to obtain feasible values of the transparent impedance along the entire horn.

It is noted that the use of thinner substrates is also possible in principle, but it would require the use of patches with higher capacitance, which, in turn, would imply a narrower bandwidth for the metahorn.

E. Radiation Patterns for Truncated Mode

It is interesting to investigate the radiated field obtained by truncating the conical unimodal horn. To this end, the equivalence principle is applied to a spherical cap passing through the rim of the truncated cone [see Fig. 5(b)] [17].

To validate the solution obtained with the modal adiabatic currents, a full-wave MoM body of revolution (MoM-BoR) analysis method with penetrable impedance BCs has been applied to the analysis of the same structure [28]. In the MoM-BoR formulation, the field of the TE_{11} mode at the horn throat is used as excitation, while the MTS is represented with a homogenized transparent impedance tensor over a grounded slab with $\varepsilon_r = 3.4$ [see Fig. 5(d)]. The agreement between the results obtained with the two methods reveals the accuracy of the adiabatic mode model as well as the capability of the MTS to filter out spurious modal components deriving from the TE_{11} excitation. In particular, full-wave simulations confirm that the chosen impedance profile is able to provide a very low cross-polar horn. Note that the adiabatic modal currents on the spherical cap rigorously predict zero cross polar components.

III. Metahorn Design With HE_{11} Modal Reactance

A. Impedance Design With Metallic Patterning

The transparent impedance walls are next implemented in practice through the design of subwavelength cross-slotted patches printed on the grounded dielectric slab. Examples of the implemented unit cells are represented in Fig. 6. The two arms of the cross slots etched in the patches may have different lengths in order to independently control the TE-TE and TM-TM components of the MTS tensor.

It is worth noting that being the desired impedance only dependent on r, the cell geometries differ along the radial horn profile, while they do not change in the azimuthal direction.

The identification of the unit cell geometry needed to get the desired transparent impedance is based on two assumptions: 1) a local planar periodicity with a triangular lattice

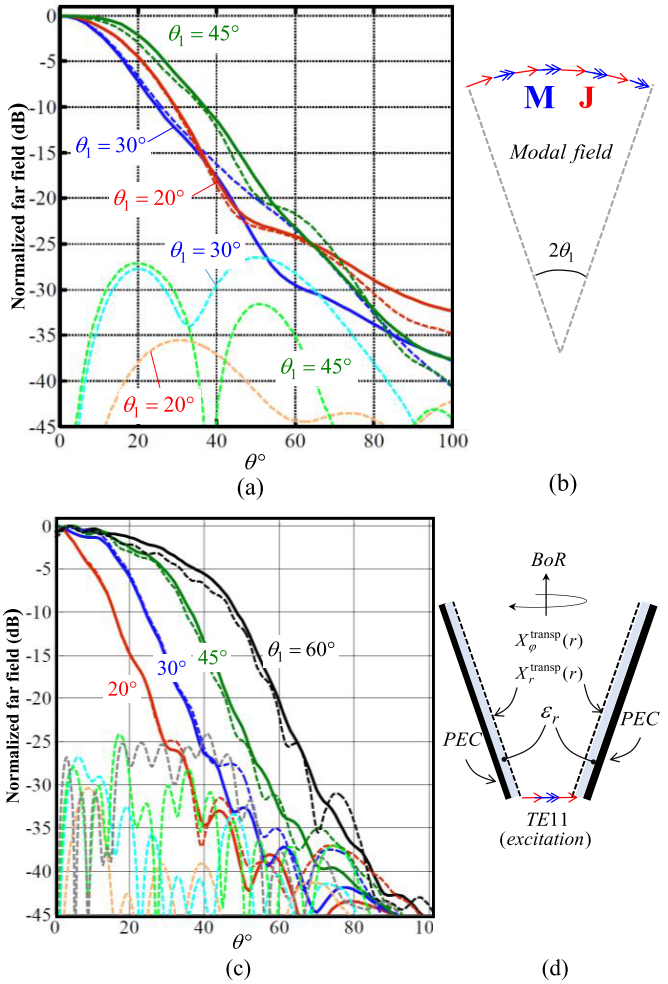

Fig. 5. Normalized far-field radiation patterns as a function of the observation angle θ; comparison of two methods for various flare angles. (a) $r_{max} = 3\lambda$. (c) $r_{max} = 10\lambda$ (results obtained at 15 GHz). Solid lines: results obtained with equivalent modal currents over the aperture cap radiating in free space (b) and dashed lines: MoM-BoR results obtained with homogenized transparent reactance sheet impedance over a grounded dielectric slab (d). Excitation is provided by using field of a TE_{11} in the circular waveguide.

and 2) a planar unit cell and a rectangular patch contour. Assumption 1 means that in each individual position, a patch is surrounded by identical patches, periodically distributed on a triangular (skew) lattice. This allows for the use of an MoM based on periodic boundary conditions. Concerning Assumption 2, it consists in approximating the curved surface on which each patch is printed with a planar one, and the slightly trapezoidal shape of each patch with a rectangular shape. This is done by a geometrical projection over the tangent plane in each point.

The skewness of the lattice in 1 [see Fig. 6(c)] is fundamental for the accuracy of the impedance extraction. Indeed, accommodating an integer number of patches over azimuthal rings implies a different number of patches in radially contiguous rings; in turn, this implies a small misalignment between neighboring patches that can be adapted to a local periodicity only with a skew angle of the local lattice.

The geometry of the unit cell is depicted in Fig. 6. The period along the radial direction Dr is kept constant and equal to 5.2 mm ($\sim\lambda/5$); the period along the azimuthal

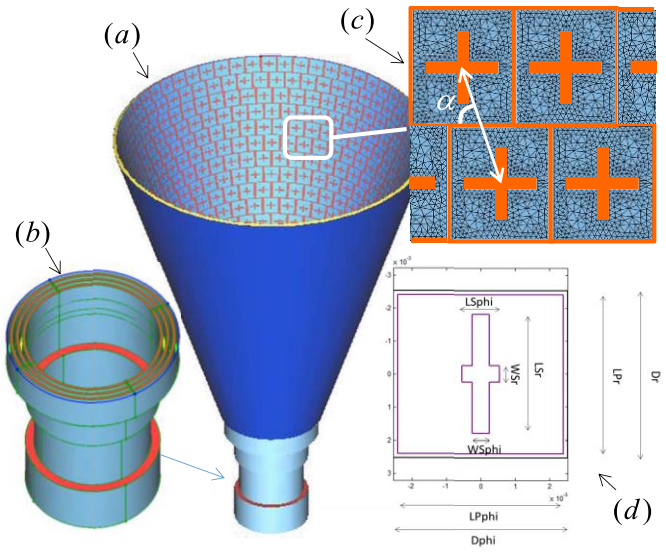

Fig. 6. (a) Numerical model of the horn with MTS constituted by metallic subwavelength patches with etched cross slots. (b) Circular waveguide transition with longitudinal corrugations. (c) Local planar periodic problem with triangular lattice and mesh. (d) Geometric parameters of the individual cell for the surface impedance database construction by periodic MoM.

direction *Dphi* is slightly varied around this value so as to accommodate an integer number of unit cells in each ring, ranging from 5.13 to 5.33 mm. From the theoretical model, each ring is characterized by an objective impedance and an incidence angle of the plane wave. Furthermore, the skewness angle of the lattice is determined by the unit cell period. In order to determine the right geometry of a local patch providing the desired value of impedance, a database has been constructed by analyzing unit cells with different geometries with a periodic MoM. The geometrical parameters involved in the database construction are the two lengths of the arms of the cross slot (*LSphi* and *LSr*) and the skewness angle of the lattice. The size of the patches, *LPphi* and *LPr,* slightly varies in each ring (*LPphi* ranges from 4 to 4.4 mm and *LPr* from 4.8 to 4.9 mm); the slot widths are kept constant and are equal to $WSphi = WSr = 0.51$ mm.

A relationship among the parameters and the values of the opaque impedance entries is established. The transparent reactance X_r, X_ϕ is individuated through a TE-TM two-port transmission line model, excited by a plane wave coming from the modal incidence angle (see Fig. 7). The transmission line model is limited to the dominant Floquet-wave mode of the local periodicity, while the higher order modes are incorporated in the equivalent transparent reactance. The database is first constructed with a coarse sampling of the parameters values and next interpolated to get continuous variations. The research of the optimal set of geometrical parameters that realizes a given couple of reactance entries is done by an optimization algorithm. The research of the optimal value is facilitated by using the geometry of contiguous patches as an entry guess. We note that the required transparent impedance matrix is diagonal; since, in general, the skewed lattice may create a small coupling among the polarizations, this coupling must be compensated by acting on the degrees of freedom of the unit cell.

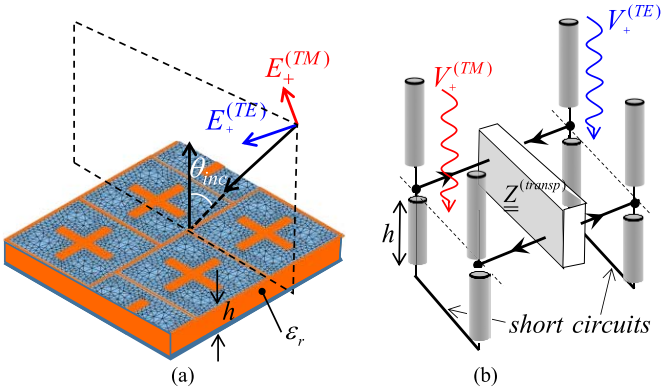

Fig. 7. (a) Local plane-wave incidence with modal incidence angle over the local flat MTS. (b) Transmission line equivalent network for the retrieval of the anisotropic modal impedance.

TABLE I
GEOMETRICAL PARAMETERS OF THE LAUNCHING SECTION

wg_{in}	wg	d_1	r_1	r_2	r_3	r_4
11.9 mm	15.24 mm	10.37 mm	12.4 mm	13 mm	13.5 mm	14.10 mm
r_5	$hcwg_1$	$hcwg_2$	$hcwg_3$	h_1	h_2	h_3
14.6 mm	10 mm	12.6 mm	15.96 mm	3.85 mm	7.95 mm	6.49 mm

B. Launcher

In order to emulate the hybrid port of the conical horn, the mode-launching region of the horn must be designed to transform a TE_{11} mode at the input circular waveguide into a hybrid HE_{11} mode at its output section (horn throat). The longitudinal profile of the final structure is reported in Fig. 8. The optimized values of the geometrical parameters are reported in Table I.

C. Full-Wave MLFMM Analysis

The final design in Fig. 8 has been analyzed by two software codes: a code by IDS based on a multilevel fast multiple method (MLFMM) [29] and the aforementioned BoR-MoM code based on homogenized transparent impedance [see Fig. 5(d)]. The results shown in Fig. 9 present the final comparison among the results obtained by the MLFMM, the BoR-MoM, and the modal currents over the aperture-cap radiating in free space [like in Fig. 5(b)]. The MLFMM results are obtained by exciting the circular waveguide cross section with a horizontal dipole, while the results from BoR-MoM have been obtained by exciting the circular waveguide section with a TE11 mode. Surprisingly, it is seen that the results by the modal aperture currents predict accurate co-polar pattern up to -10 dB from the maximum. The accuracy of the BoR-MoM analysis is also surprising, since the analysis is based on homogenized theoretical values of the impedance surface.

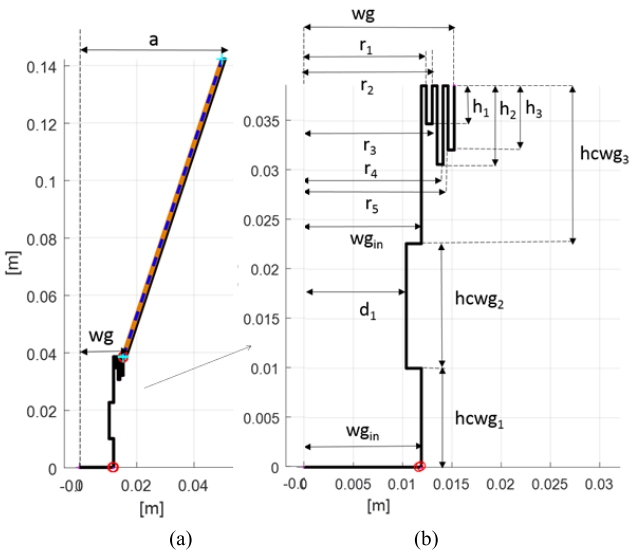

Fig. 8. Longitudinal profile of (a) horn with semi-flare angle 18.445°, a = 49.8 mm, wg = 15, 24 mm, and (b) launcher section. The values of the parameters for the launching section are reported in Table I.

Fig. 10. Final metahorn engineering model.

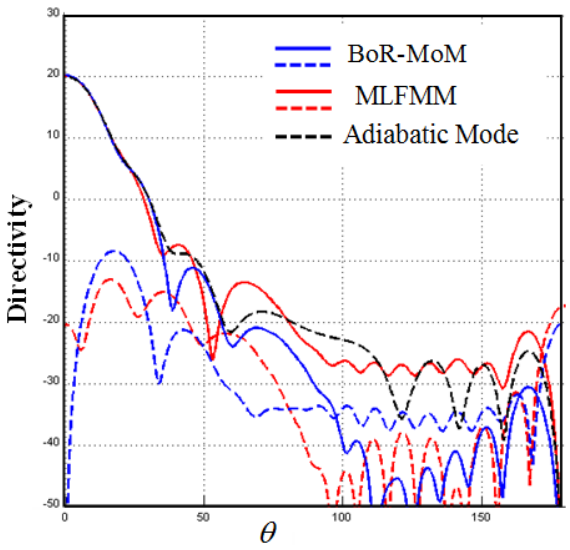

Fig. 9. Comparisons of the radiation patterns obtained from various numerical models for the final geometry in Fig. 8.

IV. Manufacturing and Measurements

A. Manufacturing

The realized conical metahorn is shown in Fig. 10. It has been realized by using a flexible substrate on which the MTS is printed. An intermediate rigid dielectric substrate machined to conical shape is placed between the MTS and the metallic wall. The outer conical horn is made of aluminum alloy and it is manufactured by means of a traditional computer numerically controlled (CNC) turning machine. Several materials have been traded-off for the intermediate conical slab. The most appropriate resulted to be ULTEM 2300 [30], an amorphous thermoplastic polymer which combines mechanical, thermal, and electrical properties. According to measurements conducted with a WR75 waveguide setup on two material samples, dielectric relative permittivity is 3.62 at X-band, and loss tangent varies between 0.029 and 0.050 in the frequency range 10–15 GHz. This has been bonded onto the inner wall of the metallic horn. The flexible substrate is DuPont Pyralux AP8545R [31]. This material is a copper-clad laminate based on a polyimide film bonded to copper foil. Among its main characteristics, this material is flexible, highly reliable, and temperature resistant. The thickness chosen for the substrate is 4 mils (100 μm), the relative dielectric constant is 3.3 at X-band, and the loss tangent is 0.004.

The substrate has been printed in plane by a photolithographic process and curved and bonded over the rigid dielectric part in autoclave with the help of a conical mold. The total thickness of the dielectric slab and the flexible printed circuit board matches the nominal design value of 1 mm. The transition between the circular waveguide and the conical horn is done by CNC turning machine and fastened to the conical part with a precision flange. The metallic launcher is composed by several axial corrugations (see Fig. 8). A commercial Ortho-Mode Transducer (OMT) is connected to the corrugated launcher in order to feed the two linear polarizations (H/V) of the conical horn with high purity and port-to-port decoupling.

B. Measurements

Scattering parameters of the manufactured horn have been measured in a fully anechoic chamber at Microwave Vision Group (MVG) (Pomezia, Italy) using an Anritsu Vector Analyzer (MS4647B). The accuracy of the test setup is ±0.05 dB at −0.5 dB levels and ±1 dB at −30 dB levels. The radiation pattern has been measured with the MVG Star Lab 18 spherical near field (SNF) antenna test range [32] (see Fig. 11), equipped with 14 probes in the range 6–18 GHz and mounted with equal spacing on a circular arch. The geometry of the setup ensures minimum interference and low ripple on the radiation patterns. The measured S-parameters at the input coaxial ports of the horn, including the OMT, are shown

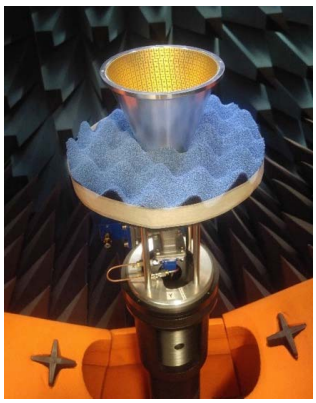

Fig. 11. Antenna under test in the MVG Star Lab 18 SNF antenna test range.

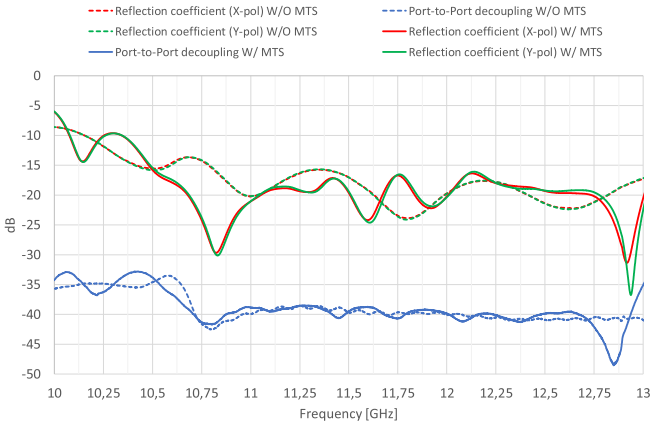

Fig. 12. Scattering parameters at the input ports of the bare metallic horn (dashed lines) and of the metahorn (continuous lines).

in Fig. 12. The resulting operational bandwidth, considering −15 dB reflection coefficient, ranges from 10.5 to 13 GHz, with a port-to-port decoupling better than −35 dB. These achieved results widely cover the expected frequency range. For the sake of comparison, the same figure also reports the reflection coefficient for the same conical horn without MTS, i.e., with bare metallic walls. As it can be seen, the presence of the MTS does not degrade the input port matching and the port-to-port decoupling.

Sample results of the measured RHCP and LHCP radiation patterns are shown in Fig. 13 in the frequency range 10.7–12.5 GHz. These results are obtained by measuring the two linear polarizations of the horn independently and then computing the resulting circular polarization in postprocessing, assuming ideal feeding with equal amplitude and phase quadrature between the coaxial ports. To minimize the impact of the OMT unidealities on the measured axial ratio, its channel imbalance between ports is calibrated out.

The plots shown in Fig. 13 also present the numerical results calculated with MLFMM tool from IDS, showing a good agreement in a range of −30 dB level. The adiabatic mode simple prediction (not shown here for not overcrowding the pictures) actually shows an accuracy over −30 dB from the co-polar components, namely of the same order of

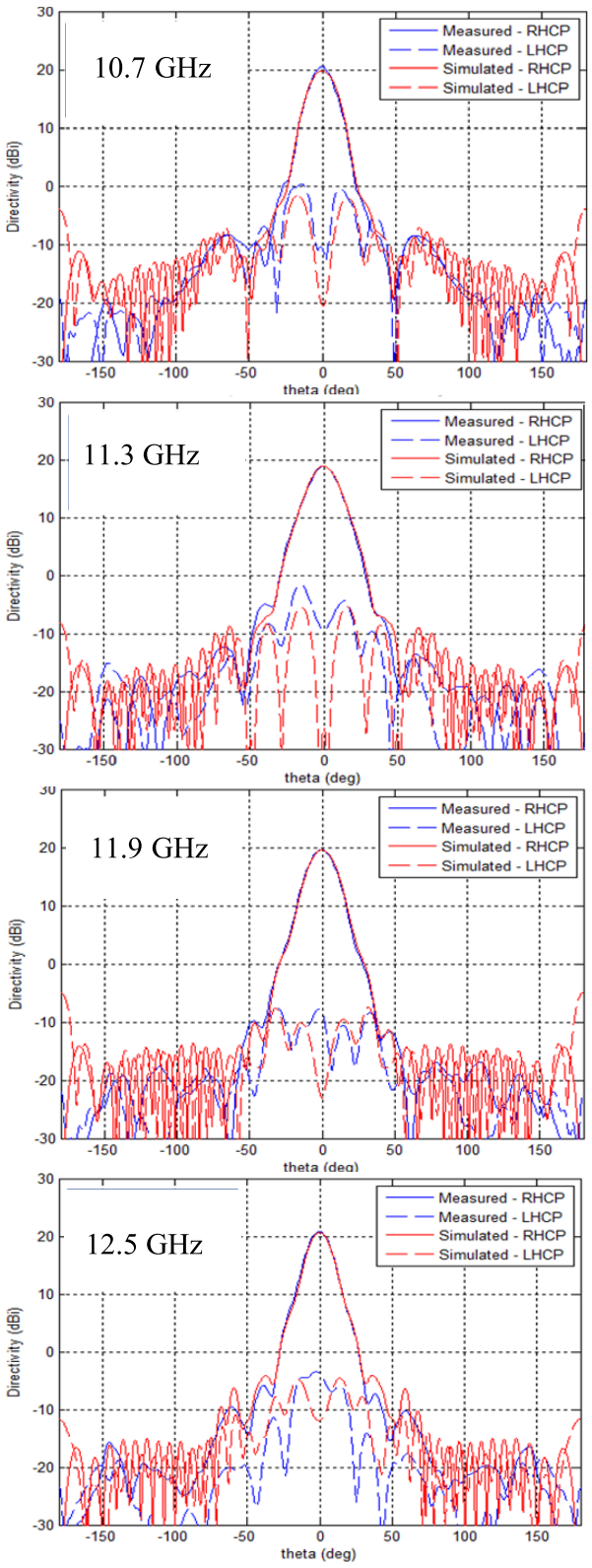

Fig. 13. Directivity patterns at various frequencies; comparison between measurements and simulation (MLFMM, IDS code).

those in Fig. 9. This confirms the validity of the extremely simplified method as an effective and reliable design tool for the initial sizing of the structure. The overall performances in the operational bandwidth are illustrated in Figs. 14–17.

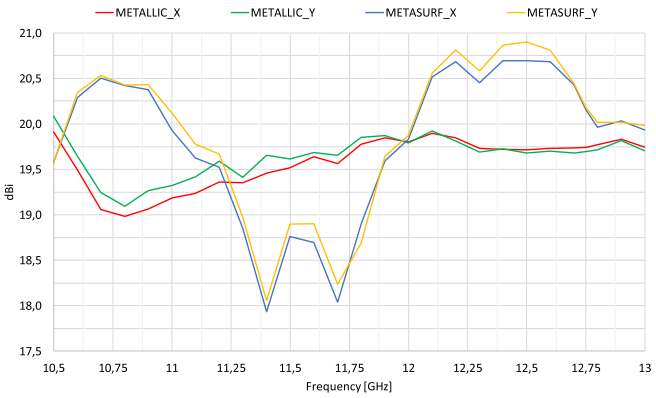

Fig. 14. Measured maximum directivity as a function of frequency for the proposed metahorn prototype and for the same horn without MTS.

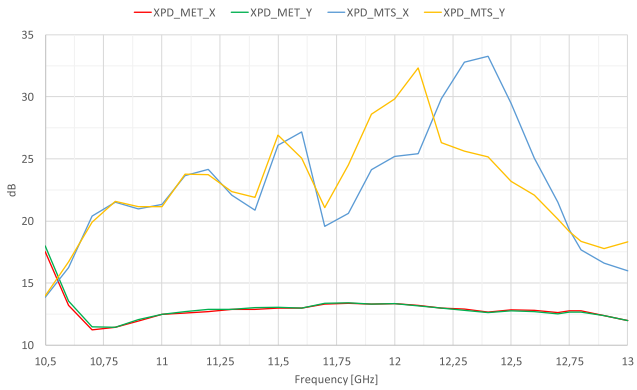

Fig. 15. Measured XPD as a function of frequency for the proposed metahorn prototype and for the same horn without MTS.

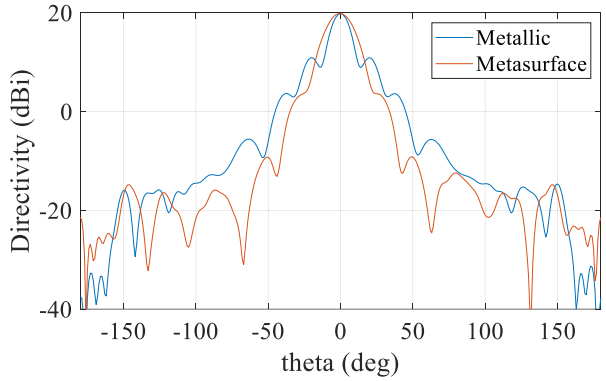

Fig. 16. Measured co-polar pattern in the E-plane at 12 GHz for the proposed metahorn prototype and for the same horn without MTS.

In particular, Fig. 14 reports the maximum directivity, Fig. 15 the minimum difference between the cross-polar field and the maximum co-polarized field, and Fig. 17 the radiation efficiency. In order to better highlight the improvement introduced by the MTS, the performance of the metallic horn without MTS is also reported in the same figures.

Cross-polar discrimination (XPD) has been calculated as the difference between the co-polar component at broadside and the maximum value of the cross-polar component in the main beam angular region $|\theta| < 17°$. It is seen that between

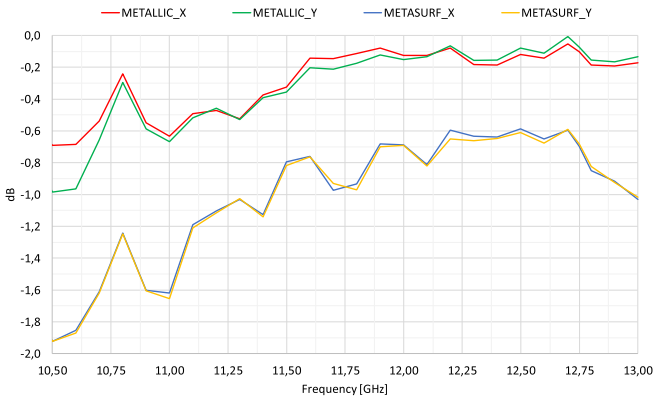

Fig. 17. Measured radiation efficiency as a function of frequency for the proposed metahorn prototype (blue and yellow lines) and for the same horn without MTS (red and green lines).

11 and 13 GHz, the cross-polar level is 25 dB below peak in average, with minima beyond 30 dB. These levels are comparable with the achievable performance of a generic corrugated horn. The improvement with respect to the bare metallic horn is around 10 dB.

On the other hand, the insertion of the MTS implies a slight decrease of the radiation efficiency (between 0.5 and 1 dB), mainly due to dielectric losses. This aspect could be improved by selecting materials with a lower loss tangent.

Finally, in order to show the improvement introduced by the MTS in the sidelobe level, co-polar radiation patterns in the E-plane (X-polarization) are shown in Fig. 16 for both the metahorn and the bare metallic horn. As it can be seen, SLL is significantly improved in the presence of the MTS. A similar behavior is also found at the other frequencies of the operational band.

V. Conclusion

A low cross-polarization conical horn based on thin MTS walls is presented. The design is performed by emulating with printed MTSs the boundary condition supporting the HE11 mode in a conical waveguide with AIBCs on the walls. These BCs exhibit $1/r$ and r dependencies for the two components of the tensor impedance, and they support a mode perfectly balanced in polarization. The tensor impedance is implemented by printing patches with two slots over a grounded slab, without using any optimization method for correcting the impedance. With respect to previously published solutions for metahorn implementation, the one proposed in this article is simpler to manufacture since no vertical metallizations are required and it offers the advantage of thinner walls and reduced mass with respect to a corrugated horn. These characteristics, combined with the possibility to shape the radiation pattern by redesigning the MTS, make the proposed design particularly suitable for space applications, where performance requirements are demanding, and mass and bulkiness reduction are of primary importance. The final measurements of a 20 dB gain *Ku*-band prototype have evidenced a cross-polar level below -20 dB over 2 GHz bandwidth around 12 GHz, with a best performance of less than -30 dB.

ACKNOWLEDGMENT

The authors wish to thank the other participants to the ARTES project "High-performance horns with customisable radiation properties", in particular R. Ravanelli, Thales Alenia Space, Italy, A. Francavilla, Istituto Superiore Mario Boella, L. Foged, Microwave Vision Group, Italy, and the company GERG GmbH for manufacturing of the engineering model.

REFERENCES

[1] P. D. Potter, "A new horn antenna with suppressed sidelobes and equal beamwidth," *Microw. J.*, vol. 6, pp. 71–78, Jun. 1963.

[2] A. J. Simmons and A. F. Kay, "The scalar feed—A high performance feed for large paraboloid reflectors," in *Design and Construction of Large Steerable Aerials*, vol. 21. 1966, pp. 213–217.

[3] H. Minnett and B. Thomas, "A method of synthesizing radiation patterns with axial symmetry," *IEEE Trans. Antennas Propag.*, vol. 14, no. 5, pp. 654–656, Sep. 1966.

[4] P. J. B. Clarricoats and A. D. Olver, *Corrugated Horns for Microwave Antennas* (Electromagnetic Waves). London, U.K.: Peregrinus, 1984, ch. 3.

[5] V. Rumsey, "Horn antennas with uniform power patterns around their axes," *IEEE Trans. Antennas Propag.*, vol. AP-14, no. 5, pp. 656–658, Sep. 1966.

[6] P. S. Kildal, E. Lier, and J. A. Aas, "Artificially soft and hard surfaces in electromagnetics and their application," in *Antennas Propag. Soc. Int. Symp. Dig. (AP-S)*, Syracuse, NY, USA, 1988, pp. 832–835.

[7] E. Lier and P.-S. Kildal, "Soft and hard horn antennas," *IEEE Trans. Antennas Propag.*, vol. AP-36, no. 8, pp. 1152–1157, Aug. 1988.

[8] E. Lier, "Review of soft and hard horn antennas, including metamaterial-based hybrid-mode horns," *IEEE Antennas Propag. Mag.*, vol. 52, no. 2, pp. 31–39, Apr. 2010.

[9] E. Lier, "Hybrid-mode horn antenna with design-specific aperture distribution and gain," in *Proc. IEEE Int. Symp. Antennas Propag.*, Columbus, OH, USA, Jun. 2003, pp. 502–505.

[10] E. Lier and A. Kishk, "A new class of dielectric-loaded hybrid-mode horn antennas with selective gain: Design and analysis by single mode model and method of moments," *IEEE Trans. Antennas Propag.*, vol. 53, no. 1, pp. 125–138, Jan. 2005.

[11] E. Lier, D. H. Werner, and T. S. Bird, "The evolution from metal horns to metahorns: The development of EM horns from their inception to the present day," *IEEE Antennas Propag. Mag.*, vol. 61, no. 4, pp. 6–18, Aug. 2019.

[12] S. Maci, G. Minatti, M. Casaletti, and M. Bosiljevac, "Metasurfing: Addressing waves on impenetrable metasurfaces," *IEEE Antennas Wireless Propag. Lett.*, vol. 10, pp. 1499–1502, 2011.

[13] M. Bosiljevac, M. Casaletti, F. Caminita, Z. Sipus, and S. Maci, "Non-uniform metasurface luneburg lens antenna design," *IEEE Trans. Antennas Propag.*, vol. 60, no. 9, pp. 4065–4073, Sep. 2012.

[14] E. Lier and R. K. Shaw, "Design and simulation of metamaterial-based hybrid-mode horn antennas," *Electron. Lett.*, vol. 44, no. 25, p. 1444, 2008.

[15] Q. Wu, C. P. Scarborough, D. H. Werner, E. Lier, and X. Wang, "Design synthesis of metasurfaces for broadband hybrid-mode horn antennas with enhanced radiation pattern and polarization characteristics," *IEEE Trans. Antennas Propag.*, vol. 60, no. 8, pp. 3594–3604, Aug. 2012.

[16] Q. Wu, C. P. Scarborough, D. H. Werner, E. Lier, and R. K. Shaw, "Inhomogeneous metasurfaces with engineered dispersion for broadband hybrid-mode horn antennas," *IEEE Trans. Antennas Propag.*, vol. 61, no. 10, pp. 4947–4956, Oct. 2013.

[17] P. J. Clarricoats and P. K. Saha, "Propagation and radiation behavior of corrugated feeds," *Proc. Inst. Elect. Eng.*, vol. 118, pp. 1167-1186, Sep. 1971.

[18] A. D. Olver and J. Xiang, "Wide angle corrugated horns analysed using spherical modal-matching," *IEE Proc. H, Microw., Antennas Propag.*, vol. 135, no. 1, pp. 34–40, 1988.

[19] V. Sozio *et al.*, "Low cross polarization conical metahorn based on an adiabatic mode formulation," in *Proc. 11th Eur. Conf. Antennas Propag. (EuCAP)*, Paris, France, Mar. 2017, pp. 19–24.

[20] E. Martini, M. Mencagli, and S. Maci, "Metasurface transformation for surface wave control," *Phil. Trans. Roy. Soc. A, Math., Phys. Eng. Sci.*, vol. 373, no. 2049, Aug. 2015, Art. no. 20140355.

[21] J. Pearson, "Computation of hypergeometric functions," M.S. thesis, Math. Model. Sci. Comput. Univ. Oxford, Oxford, U.K., Sep. 2009.

[22] J. Pearson. *MATLAB Routines for the Computation of Hypergeometric*. Accessed: 2014. [Online]. Available: http://people.maths.ox.ac.uk/porterm/research/hypergeometricpackage.zip

[23] J. M. Arnold and A. Dendane, "Intrinsic mode theory of conical corrugated horns," *IEE Proc. H-Microw., Antennas Propag.*, vol. 136, no. 3, pp. 250–256, Jun. 1989.

[24] L. B. Felsen and L. Sevgi, "Adiabatic and intrinsic modes for wave propagation in guiding environments with longitudinal and transverse variation: Formulation and canonical test," *IEEE Trans. Antennas Propag.*, vol. 39, no. 8, pp. 1130–1136, Aug. 1991.

[25] A. D. Olver, P. J. B. Clarricoats, and L. Shafai, *Microwave Horns and Feeds*. London, U.K.: Institution Electrical Engineering, 1994.

[26] A. Tellechea Pereda *et al.*, "Dual circularly polarized broadside beam metasurface antenna," *IEEE Trans. Antennas Propag.*, vol. 64, no. 7, pp. 2944–2953, Jul. 2016.

[27] M. Mencagli, E. Martini, and S. Maci, "Transition function for closed-form representation of metasurface reactance," *IEEE Trans. Antennas Propag.*, vol. 64, no. 1, pp. 136–145, Jan. 2016.

[28] F. Caminita, M. Faenzi, D. G. Ovejero, and S. Maci, "Numerical issues in the analysis of large BoR antennas involving dielectric and metallic parts," in *Proc. 7th Eur. Conf. Antennas Propag. (EuCAP)*, Gothenburg, Sweden, 2013, pp. 4043–4045.

[29] *GALILEO Suite Website*. Accessed: 2019. [Online]. Available: https://www.idscorporation.com/pf/galileo-suite

[30] *SABIC Website*. Accessed: May 2019. [Online]. Available: https://www.sabic.com/en

[31] *DuPont Pyralux AP8545R Datasheet*. Accessed: May 2019. [Online]. Available: https://www.dupont.com/content/dam/dupont/products-and-services/electronic-and-electrical-materials/flexible-rigid-flex-circuit-materials/documents/PyraluxAPclad_DataSheet.pdf

[32] *MVG StarLab 18 GHz Datasheet*. Accessed: Feb. 2020. [Online]. Available: https://www.mvg-world.com/sites/default/files/2019-10/Datasheet_Antenna%20Measurement_StarLab_EN_10_19_BD.pdf

Valentina Sozio received the M.Sc. degree in telecommunications engineering from "La Sapienza" University of Rome, Rome, Italy, in 2009, and the Ph.D. degree in engineering and science of information from the University of Siena, Siena, Italy, in 2015, investigating 3-D metamaterials homogenization techniques.

In 2014, during a six-month period spent at the Université catholique de Louvain, Ottignies-Louvain-la-Neuve, Belgium, her research focused on numerical methods for metamaterials characterization. From 2015 to 2019, she worked in Turin, first at the Istituto Superiore Mario Boella and then at LINKS Foundation, where she was involved in antenna design projects.

Enrica Martini (Senior Member, IEEE) received the Laurea degree (*cum laude*) in telecommunication engineering from the University of Florence, Florence, Italy, in 1998, and the Ph.D. degree in informatics and telecommunications from the University of Florence and the Ph.D. degree in electronics from the University of Nice Sophia Antipolis, Nice, France, in 2002, under joint supervision.

In 2002, she was appointed as a Research Associate with the University of Siena, Siena, Italy. In 2005, she received the Hans Christian Ørsted Post-Doctoral Fellowship from the Technical University of Denmark, Lyngby, Denmark, and she was with the Electromagnetic Systems Section, Ørsted•DTU Department, until 2007. From 2007 to 2017, she was a Post-Doctoral Fellow with the University of Siena. From 2016 to 2018, she was the CEO of the startup Wave Up Srl, Siena, which she co-funded in 2012. She is currently an Assistant Professor with the University of Siena. She worked under a one-year research grant in Alenia Aerospazio Company, Rome, Italy, until 1999, in the University of Florence. Her research interests include metasurfaces and metamaterials, electromagnetic scattering, antenna measurements, finite-element methods, and tropospheric propagation.

Dr. Martini was a co-recipient of the 2016 Schelkunoff Transactions Prize Paper Award and the Best Paper Award in Antenna Design and Applications at the 11th European Conference on Antennas and Propagation.

Francesco Caminita received the M.Sc. degree (*cum laude*) in telecommunication engineering and the Ph.D. degree in information engineering from the University of Siena, Siena, Italy, in 2005 and 2009, respectively.

From 2006 to 2014, he was an Associate Researcher with the Department of Information Engineering and Mathematics, University of Siena. Since 2014, he has been with Wave Up Srl, Siena, where he is currently the CTO. He is a principal author or coauthor of over ten articles and over 50 articles in the proceedings of international conferences. His main expertise is in the area of periodic structures, frequency-selective surfaces, electromagnetic bandgap structures, artificial surfaces, and holographic antennas, including beadboard design for metasurface-based antennas, reconfigurable metasurface antennas, and mechanical implementation of antenna RF design.

Dr. Caminita was a co-recipient of the Best Paper Award on Antenna Theory at the 5th European Conference on Antennas and Propagation (EuCAP) and the 2016 Schelkunoff Transactions Prize Paper Award.

Paolo De Vita received the M.S. degree in electronic engineering and the Ph.D. degree in information and telecommunication engineering from the University of Florence, Florence, Italy, in 1999 and 2004, respectively.

From 1999 to 2007, he has served as a Research Assistant with the Department of Electronics and Telecommunication, University of Florence. Since 2008, he has been with Ingegneria dei Sistemi (IDS), Pisa, Italy. His main research interests are on numerical techniques for electromagnetic radiation and scattering problems.

Marco Faenzi was born in Siena, Italy. He received the M.Sc. degree in telecommunications engineering (with a score of 110/110) and the Ph.D. degree from the Department of Information Engineering and Mathematics, University of Siena, Siena, in 2011 and 2015, respectively. His Ph.D. was focused on the development of high-gain apertures for space applications based on modulated metasurface structures realized by inductive or capacitive textures.

He is currently a Post-Doctoral Researcher with the Institut d'Électronique et de Télécommunications of Rennes (IETR), University of Rennes 1, Rennes, France. He has worked on metasurfaces holographic patterning for the optimization of aperture efficiency of dipole-excited planar resonator. During his post-doctoral activity, he worked toward characterization, optimization, and synthesis of modulated metasurface apertures of multifrequency and broadband operativity. He also worked toward the application of metasurface technology for the implementation of multibeam and highly efficient monopulse apertures in linear and circular polarizations.

Dr. Faenzi was a co-recipient of the Sergei A. Schelkunoff Transactions Prize Paper Award by the IEEE Antennas and Propagation Society in 2016. In 2015, he won a co-financed Post-Doctoral Grant in the Networking/Partnering Initiative Framework by the European Space Agency and the University of Siena.

Andrea Giacomini (Member, IEEE) was born in Rome, Italy, in 1977. He received the M.Sc. degree in electrical engineering from the University of Rome Tor Vergata, Rome, in 2002.

Since his master's thesis, he has been with SATIMO and later Microwave Vision Italy s.r.l., Pomezia, Italy, first as an Antenna Engineer and then as an Antenna Department Manager. He has authored or coauthored more than 50 journal articles and conference papers on antenna design and measurement topics and holds two patents in microwave orthomode junctions. His professional interests and research activities relate to antenna design and measurement techniques. In particular, he is involved in the development of reference antennas, wideband radiators, measurement probes for planar near field/spherical near field (PNF/SNF) applications, Compact Antenna Test Range (CATR) feeds, and passive microwave components, such as orthomode junctions and beam-forming networks. He is also actively involved in several ESA programs focused on novel antenna concepts for space applications.

Marco Sabbadini received the M.Sc. degree from the Università di Roma Sapienza, Rome, Italy, in 1983.

From 1983 to 1988, he was with the Antenna Group, Thales Alenia Space Italy, Rome. From 1988 to 2018, he was with the European Space Agency, ESTEC, Noordwijk, The Netherlands. He currently collaborates with the Università di Siena, Siena, Italy. His current research interests include computational electromagnetics and computer-aided antenna engineering tools, and the development of creative solutions in space antenna technology, and most notably, the recent development of modulated metasurface antennas. Finally, he is involved in the assessment of the impact of the plasma generated by shock waves during hypersonic atmospheric reentry on antenna radiation patterns.

Stefano Maci (Fellow, IEEE) received the Laurea degree (*cum laude*) in electronics engineering from the University of Florence, Florence, Italy, in 1987.

Since 1997, he has been a Professor with the University of Siena, Siena, Italy. He has coauthored over 150 articles published in international journals, among which 100 are in the IEEE journals, ten book chapters, and about 400 articles in the proceedings of international conferences. These articles have received around 6700 citations. His current research interests include high-frequency and beam representation methods, computational electromagnetics, large phased arrays, planar antennas, reflector antennas and feeds, metamaterials, and metasurfaces.

Prof. Maci was a former member of the IEEE AP-S AdCom, the EurAAP Board of Directors, and the Antennas and Propagation Executive Board of the Institution of Engineering and Technology, U.K. He was a recipient of the European Association on Antennas and Propagation (EurAAP) Award in 2014, the Sergei A. Schelkunoff Transactions Prize Paper Award, and the Chen-To Tai Distinguished Educator Award from the IEEE Antennas and Propagation Society (IEEE AP-S) in 2016. Since 2000, he has been a member of the Technical Advisory Board of 11 international conferences and the Review Board of six international journals. He has organized 25 special sessions in international conferences and held ten short courses in the IEEE AP-S Symposia about metamaterials, antennas, and computational electromagnetics. In 2004, he was the Founder of the European School of Antennas, a post-graduate school that presently comprises 30 courses on antennas, propagation, electromagnetic theory, and computational electromagnetics, with 150 teachers from 15 countries. From 2004 to 2007, he was a WP Leader of the Antenna Center of Excellence (ACE, FP6-EU) and the International Coordinator of a 24-Institution Consortium of a Marie Curie Action (FP6) from 2007 to 2010. Since 2010, he has been a Principal Investigator of six cooperative projects financed by the European Space Agency. He has been the Director of the University of Siena's Ph.D. Program in information engineering and mathematics from 2008 to 2015 and a member of the National Italian Committee for Qualification to Professor from 2013 to 2015. He is the Director of the consortium FORESEEN, which currently consists of 48 European institutions, and a Principal Investigator of the Future Emerging Technology project Nanoarchitectronics of the 8th EU Framework Program. He was the Co-Founder of two spin-off companies. He is a Distinguished Lecturer of the IEEE AP-S and of EuRAAP. He was an Associate Editor of the IEEE TRANSACTIONS ON ANTENNAS AND PROPAGATION and the Chair of the Award Committee of the IEEE AP-S.

Giuseppe Vecchi (Fellow, IEEE) received the Laurea and Ph.D. (Dottorato di Ricerca) degrees in electronic engineering from the Politecnico di Torino, Turin, Italy, in 1985 and 1989, respectively, with doctoral research carried out partly at Polytechnic University, Farmingdale, NY, USA.

He was a Visiting Scientist with Polytechnic University from 1989 to 1990. Since 1990, he has been with the Department of Electronics, Politecnico di Torino, as an Assistant Professor, an Associate Professor in 1992, and a Professor since 2000, where he is currently the Director of the Antenna and Electromagnetic Compatibility Laboratory. He was also a Visiting Scientist with the University of Helsinki, Helsinki, Finland, in 1992 and an Adjunct Faculty Member with the Department of Electrical and Computer Engineering, University of Illinois at Chicago, Chicago, IL, USA, from 1997 to 2011. His current research activities concern analytical and numerical techniques for analysis, design, and diagnostics of antennas and devices, and imaging.

Dr. Vecchi is a member of the Board of the European School of Antennas; he has been the Chairman of the IEEE AP/MTT/ED Italian joint Chapter on the IEEE-APS Educational Committee and an Associate Editor of the IEEE TRANSACTIONS ON ANTENNAS AND PROPAGATION.